PHILOSOPHICAL TRANSACTIONS A

rsta.royalsocietypublishing.org

Opinion piece

Cite this article: Winkler JR, Gray HB. 2015 Could tyrosine and tryptophan serve multiple roles in biological redox processes? *Phil. Trans. R. Soc. A* **373**: 20140178.
http://dx.doi.org/10.1098/rsta.2014.0178

One contribution of 18 to a discussion meeting issue 'The new chemistry of the elements'.

Subject Areas:
inorganic chemistry

Keywords:
electron transfer, hopping, protein radical, azurin, cytochrome P450

Author for correspondence:
Harry B. Gray
e-mail: hbgray@caltech.edu

Could tyrosine and tryptophan serve multiple roles in biological redox processes?

Jay R. Winkler and Harry B. Gray

Beckman Institute, California Institute of Technology, 1200 East California Boulevard, Pasadena, CA 91125, USA

Single-step electron tunnelling reactions can transport charges over distances of 15–20 Å in proteins. Longer-range transfer requires multi-step tunnelling processes along redox chains, often referred to as hopping. Long-range hopping via oxidized radicals of tryptophan and tyrosine, which has been identified in several natural enzymes, has been demonstrated in artificial constructs of the blue copper protein azurin. Tryptophan and tyrosine serve as hopping way stations in high-potential charge transport processes. It may be no coincidence that these two residues occur with greater-than-average frequency in O_2- and H_2O_2-reactive enzymes. We suggest that appropriately placed tyrosine and/or tryptophan residues prevent damage from high-potential reactive intermediates by reduction followed by transfer of the oxidizing equivalent to less harmful sites or out of the protein altogether.

1. Background

It is well established that multi-step tunnelling, called hopping, is required for functional charge transport in many redox enzymes (examples include ribonucleotide reductase [1–9], photosystem II [10–12], DNA photolyase [13–21], MauG [22–25] and cytochrome *c* peroxidase [26,27]). Here, we advance the hypothesis that many such enzymes, most especially those that generate high-potential intermediates during turnover, could be irreversibly damaged if the intermediates are not inactivated in some way. We suggest that appropriately placed tyrosine (Tyr) and/or tryptophan (Trp) residues can prevent such damage by rapid reduction of the intermediates followed by transfer of the oxidizing equivalent to less harmful sites or out of the protein altogether [28]. A protective role of this sort will not

THE ROYAL SOCIETY PUBLISHING

be apparent in catalytic rates and binding constants; the enzyme survival time is more likely to be an indicator of this function.

The blue copper protein *Pseudomonas aeruginosa* azurin has been a test-bed for mechanistic investigations of Trp and Tyr radical formation in biological electron transfer (ET) reactions [29–33]. Our initial investigations revealed that Cu^{I} oxidation by a photoexcited Re^{I}-diimine ($Re^{I}(CO)_3(dmp)$, dmp = 4,7-dimethyl-1,10-phenanthroline) covalently bound at His^{124} on a $His^{124}Gly^{123}Trp^{122}Met^{121}$ β-strand ($ReHis^{124}Trp^{122}Cu^{I}$-azurin) occurs in a few nanoseconds, fully two orders of magnitude faster than documented for single-step electron tunnelling at a 19 Å donor–acceptor distance [29]. We attributed the accelerated ET to a two-step hopping mechanism involving a $Trp^{\bullet+}$ radical intermediate. In recent work, we examined ET in $ReHis^{126}Trp^{122}Cu^{I}$-azurin, which has three redox sites at well-defined distances in the protein fold (Re–Trp^{122}(indole) = 13.1 Å, dmp–Trp^{122}(indole) = 10.0 Å, Re–Cu = 25.6 Å) [32]. Near-UV excitation of the Re chromophore leads to prompt Cu^{I} oxidation (less than 50 ns), followed by slow back-ET (more than 0.2 μs) to regenerate Cu^{I} and ground-state Re^{I}. Spectroscopic measurements performed with varying protein concentrations suggest that the photoinduced ET reactions occur in protein dimers, $(ReHis^{126}Trp^{122}Cu^{I})_2$, and that forward ET is accelerated by intermolecular electron hopping through the interfacial tryptophan: $^{*}Re\| \leftarrow Trp^{122} \leftarrow Cu^{I}$ (‖ denotes a protein–protein interface). Solution mass spectrometry confirms a broad oligomer distribution with prevalent monomers and dimers, and the crystal structure of the Cu^{II} form reveals two $ReHis^{126}Trp^{122}Cu^{II}$ molecules oriented such that redox cofactors Re(dmp) and Trp^{122}-indole on different protein molecules are located in the interface at much shorter intermolecular distances (Re–Trp^{122}(indole) = 6.9 Å, dmp–Trp^{122}(indole) = 3.5 Å and Re–Cu = 14.0 Å) than within single protein folds. Whereas forward ET is accelerated by hopping through Trp^{122}, $Re^{I}(dmp^{\bullet-})\| \rightarrow Cu^{II}$ ET is sluggish, probably due to poor electronic coupling across the protein–protein interface as well as the absence of an energetically accessible radical intermediate. These findings provided new insights into the factors that regulate $Trp^{\bullet+}$ radical formation in protein ET reactions involving high-potential oxidants.

Work by theorists has shed much light on the main factors controlling biological ET reactions [34,35]: and, in our experimental programme, we have found semiclassical ET theory [36] to be particularly useful in analyses of results. Notably, given a particular spatial arrangement of redox cofactors, we can predict driving force dependences of the relative time constants for single-step ($\tau_{ss} = 1/k_{ss}$) and multi-step (τ_{hop}) electron transport [31]. Alternatively, given the redox and reorganization energetics, we can predict the hopping propensity for different cofactor arrangements [33]. We considered azurins labelled with $Ru(bpy)_2(im)(His^{X})^{2+}$ (bpy = 2,2′-bipyridine; im = imidazole; His^{X} = surface histidine) labelled at three surface sites ($RuHis^{107}$, $RuHis^{124}$ and $RuHis^{126}$) and examined the hopping advantage (τ_{ss}/τ_{hop}) for a protein with a generalized intermediate (Int) situated between a diimine-Ru^{III} oxidant and Cu^{I} [33]. In all cases, the greatest hopping advantage occurs in systems where the Int–Ru^{III} distance (r_1) is up to 5 Å shorter than the Int–Cu^{I} distance (r_2). The hopping advantage increases as systems orient nearer a linear donor–Int–acceptor configuration, owing to minimized intermediate tunnelling distances. The smallest predicted hopping advantage is in $RuHis^{124}$-azurin, which has the shortest Ru–Cu distance of the three proteins. The hopping advantage is nearly lost as ΔG° for the first step ($Ru^{III} \leftarrow Int$) rises above +0.15 eV. Isoergic initial steps provide a wide distribution of arrangements, where advantages as great as 10^4 are possible (for a fixed donor–acceptor distance of 23.7 or 25.4 Å). A slightly exergonic $Int \rightarrow Ru^{III}$ step provides an even larger distribution of arrangements for productive hopping, which will be the case as long as the driving force for the first step is not more favourable than that for overall transfer.

We tested these predictions experimentally in three Ru–His-labelled azurins using nitrotyrosinate (NO_2TyrO^{-}) as a redox intermediate ($RuHis^{107}(NO_2TyrOH)^{109}$; $RuHis^{124}(NO_2TyrOH)^{122}$; and $RuHis^{126}(NO_2TyrOH)^{122}$; $E^{\circ\prime}(NO_2TyrO^{\bullet/-}) \approx 1.02$ V versus NHE) [33]. The first two systems have cofactor placements that are close to the predicted optimum; the last system has a larger first-step distance, which is predicted to decrease the hopping advantage. The phenol pK_a of 3-nitrotyrosine (7.2) permitted us to work at near-neutral pH, rather than the

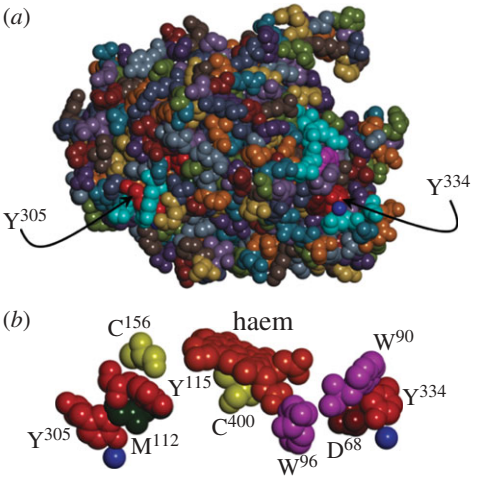

Figure 1. (*a*) Space-filling structural model of the haem domain of CYP102A1 (PDB #2IJ2) highlighting the surface locations of terminal residues in two potential radical transfer pathways (Tyr^{334} and Tyr^{305}). (*b*) Space-filling model of the residues comprising CYP102A1 putative radical transfer pathways. Blue spheres represent structurally resolved water molecules. (Online version in colour.)

high pH (more than 10) required for hopping with tyrosinate. ET via nitrotyrosinate avoids the complexities associated with the proton-coupled redox reactions of tyrosine [37–39]. We found specific rates of Cu^{I} oxidation more than 10 times greater than those of single-step ET in the corresponding azurins lacking NO_2TyrOH, confirming that NO_2TyrO^- accelerates long-range ET. In this case, the proposed reaction sequence is $[Ru^{III}\text{-}NO_2TyrO^-\text{-}Cu^{I}] \rightarrow [Ru^{II}\text{-}NO_2TyrO^{\bullet}\text{-}Cu^{I}] \rightarrow [Ru^{II}\text{-}NO_2TyrO^-\text{-}Cu^{II}]$, although the nitrotyrosyl radical intermediate was not detected by transient spectroscopy in any of the proteins investigated. The results are in excellent agreement with hopping maps developed using semiclassical ET theory and parameters derived from our body of protein ET measurements [31,33,40–42].

2. Protecting P450s?

The cytochromes P450 are members of a superfamily of haem oxygenases that perform two broad functional roles: xenobiotic metabolism and biosynthesis [43,44]. In mammals, these functions include drug metabolism, conversion of lipophilic molecules to more polar products for enhanced elimination, steroid biosynthesis and conversion of polyunsaturated fatty acids to biologically active products [43,45]. P450s are monooxygenases that incorporate one oxygen atom from O_2 into the substrate while the second is reduced to H_2O [43,44]. Substrate binding triggers reduction of the ferric enzyme to the ferrous state by a reductase with reducing equivalents originating in NAD(P)H. Oxygen binding, followed by delivery of a second electron, induces O−O bond cleavage, producing H_2O and a ferryl-porphyrin cation radical (Cmpd-1). Cmpd-1 transfers an O atom to substrate, regenerating the ferric haem [43]. The UniProtKB/Swiss-Prot database indicates that P450s are rich in aromatic amino acids: 90% of the sequences in the P450 family (956 sequences) have above-average occurrence of Phe residues; and 68% of the sequences have more Trp residues than average. Phe residues are unlikely to participate as real intermediates in ET reactions, but their role in enhanced superexchange coupling for long-range ET remains unresolved [46–48]. Cytochrome P450 BM3 (CYP102A1) is frequently used as a soluble surrogate for human microsomal P450 s [44]. A Trp^{96} residue is found within 5 Å of the haem in the structure of CYP102A1 [49] (figure 1), and sequence alignment (UniProtKB) in the P450 family suggests that Trp is conserved at this position in more than 75% of the members of this group. The most

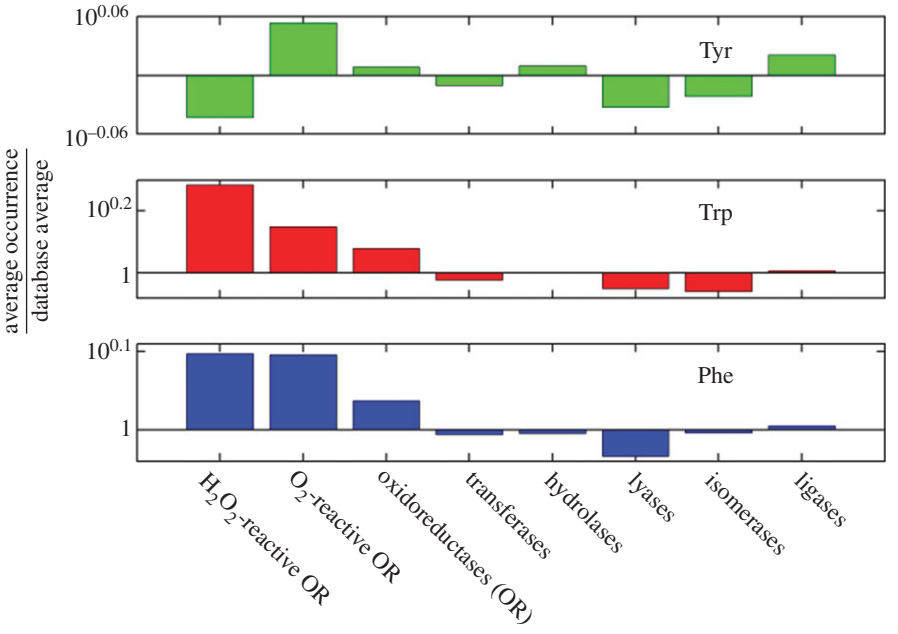

Figure 2. Occurrence frequencies relative to the UniProtKB/Swiss-Prot database average of aromatic residues (Phe, Trp and Tyr) in different enzyme classes. (Online version in colour.)

common alternative residue at this position is His. Interestingly, of the 698 sequences with Trp at this position, all but five derive from eukaryotic sources, whereas about half of the proteins with His at this position derive from bacterial or archaeal sources. The strong conservation of the Trp^{96} residue has been noted previously [50]. An ET mediator role for this residue had been suggested, but replacement of Trp^{96} with Ala, Phe or Tyr has little impact on catalytic turnover kinetics [50]. To the best of our knowledge, no role other than structural has been reported for this highly conserved Trp residue in P450 [44].

The oxygenation chemistry catalysed by some P450s is tightly coupled to substrate hydroxylation: one mole of product is produced for each mole of O_2 consumed. In many enzymes, particularly the eukaryotic proteins with broad substrate specificities, hydroxylation is much less efficiently coupled to O_2 reduction (frequently less than 10%) [51–53]. When the enzyme does not transfer an O atom to substrate, it can produce reactive oxygen species (ROS: O_2^-, H_2O_2) or a second H_2O molecule [54]. The production of ROS can lead to rapid degradation of the enzyme. In the case of oxidase chemistry (formation of $2H_2O$ from O_2), two reducing equivalents must be delivered by sources other than the substrate. Uncoupled P450 catalysis leads to oxidation of bilirubin and uroporphyrinogen [55,56]. The physiological consequences of this uncoupling could involve uroporphyria and lowered plasma bilirubin concentrations [56]. Halogenated P450 substrates, including environmental toxins such as polyhalogenated biphenyls, are associated with inhibition of monooxygenase activity and uncoupled O_2 consumption [55,56]. We suggest that redox-active Tyr and/or Trp residues in P450, quite possibly analogues of Trp^{96}, protect the enzyme from oxidative degradation during uncoupled catalysis.

3. Parting shots

Across the six enzyme classes (oxidoreductases, transferases, hydrolases, lyases, isomerases and ligases) defined by the Enzyme Data Bank of the Swiss Institute of Bioinformatics, greater than half of the oxidoreductases have Tyr and Trp frequencies above the database average (figure 2).

For the remaining five classes, most proteins have Trp frequencies below the database average, and only among the ligases does a majority of proteins have Tyr frequencies substantially above the database average. Refinement of this analysis reveals that, of the O_2-reactive oxidoreductases, 66% have Tyr frequencies above the database average and 81% have above-average Trp frequencies. Could the direct participation of Tyr and Trp residues in enzymatic redox chemistry be far more common than currently recognized? We think so!

Funding statement. Our work on biological electron transfer processes is supported by the National Institutes of Health (DK-019038) and the Arnold and Mabel Beckman Foundation.

References

1. Sjöberg BM. 1997 Ribonucleotide reductases—a group of enzymes with different metallosites and a similar mechanism. *Struct. Bonding* **88**, 139–173. (doi:10.1007/3-540-62870-3_5)
2. Stubbe J, Nocera DG, Yee CS, Chang MCY. 2003 Radical initiation in the class I ribonucleotide reductase: long-range proton-coupled electron transfer? *Chem. Rev.* **103**, 2167–2201. (doi:10.1021/cr020421u)
3. Stubbe J, van der Donk WA. 1998 Protein radicals in enzyme catalysis. *Chem. Rev.* **98**, 705–762. (doi:10.1021/cr9400875)
4. Argirevic T, Riplinger C, Stubbe J, Neese F, Bennati M. 2012 ENDOR spectroscopy and DFT calculations: evidence for the hydrogen-bond network within α2 in the PCET of *E. coli* ribonucleotide reductase. *J. Am. Chem. Soc.* **134**, 17 661–17 670. (doi:10.1021/ja3071682)
5. Holder PG, Pizano AA, Anderson BL, Stubbe J, Nocera DG. 2012 Deciphering radical transport in the large subunit of class I ribonucleotide reductase. *J. Am. Chem. Soc.* **134**, 1172–1180. (doi:10.1021/ja209016j)
6. Offenbacher AR, Minnihan EC, Stubbe J, Barry BA. 2013 Redox-linked changes to the hydrogen-bonding network of ribonucleotide reductase β2. *J. Am. Chem. Soc.* **135**, 6380–6383. (doi:10.1021/ja3032949)
7. Worsdorfer B *et al*. 2013 Function of the diiron cluster of *Escherichia coli* class Ia ribonucleotide reductase in proton-coupled electron transfer. *J. Am. Chem. Soc.* **135**, 8585–8593. (doi:10.1021/ja401342s)
8. Yokoyama K, Smith AA, Corzilius B, Griffin RG, Stubbe J. 2011 Equilibration of tyrosyl radicals ($Y_{356}^{\bullet}$, $Y_{731}^{\bullet}$, $Y_{730}^{\bullet}$) in the radical propagation pathway of the *Escherichia coli* class Ia ribonucleotide reductase. *J. Am. Chem. Soc.* **133**, 18 420–18 432. (doi:10.1021/ja207455k)
9. Offenbacher AR, Burns LA, Sherrill CD, Barry BA. 2013 Redox-linked conformational control of proton-coupled electron transfer: Y122 in the ribonucleotide reductase β2 subunit. *J. Phys. Chem. B* **117**, 8457–8468. (doi:10.1021/jp404757r)
10. Boussac A, Rappaport F, Brettel K, Sugiura M. 2013 Charge recombination in $S_nTyr_Z^{\bullet}Q_A^{-\bullet}$ radical pairs in D1 protein variants of photosystem II: long range electron transfer in the Marcus inverted region. *J. Phys. Chem. B* **117**, 3308–3314. (doi:10.1021/jp400337j)
11. Keough JM, Zuniga AN, Jenson DL, Barry BA. 2013 Redox control and hydrogen bonding networks: proton-coupled electron transfer reactions and tyrosine Z in the photosynthetic oxygen-evolving complex. *J. Phys. Chem. B* **117**, 1296–1307. (doi:10.1021/jp3118314)
12. Sjoholm J, Styring S, Havelius KGV, Ho FM. 2012 Visible light induction of an electron paramagnetic resonance split signal in photosystem II in the S_2 state reveals the importance of charges in the oxygen-evolving center during catalysis: a unifying model. *Biochemistry* **51**, 2054–2064. (doi:10.1021/bi2015794)
13. Sancar A. 2003 Structure and function of DNA photolyase and cryptochrome blue-light photoreceptors. *Chem. Rev.* **103**, 2203–2238. (doi:10.1021/cr0204348)
14. Taylor JS. 1994 Unraveling the molecular pathway from sunlight to skin cancer. *Acc. Chem. Res.* **27**, 76–82. (doi:10.1021/ar00039a003)
15. Li YF, Heelis PF, Sancar A. 1991 Active site of DNA photolyase: tryptophan-306 is the intrinsic hydrogen atom donor essential for flavin radical photoreduction and DNA repair *in vitro*. *Biochemistry* **30**, 6322–6329. (doi:10.1021/bi00239a034)
16. Aubert C, Mathis P, Eker APM, Brettel K. 1999 Intraprotein electron transfer between tyrosine and tryptophan in DNA photolysase from *Anacystis nidulans*. *Proc. Natl Acad. Sci. USA* **96**, 5423–5427. (doi:10.1073/pnas.96.10.5423)

17. Byrdin M, Eker APM, Vos MH, Brettel K. 2003 Dissection of the triple tryptophan electron transfer chain in *Escherichia coli* DNA photolyase: Trp382 is the primary donor in photoactivation. *Proc. Natl Acad. Sci. USA* **100**, 8676–8681. (doi:10.1073/pnas.1531645100)
18. Kodali G, Siddiqui SU, Stanley RJ. 2009 Charge redistribution in oxidized and semiquinone *E. coli* DNA photolyase upon photoexcitation: Stark spectroscopy reveals a rationale for the position of Trp382. *J. Am. Chem. Soc.* **131**, 4795–4807. (doi:10.1021/ja809214r)
19. Lukacs A, Eker APM, Byrdin M, Villette S, Pan J, Brettel K, Vos MH. 2006 Role of the middle residue in the triple tryptophan electron transfer chain of DNA photolyase: ultrafast spectroscopy of a Trp→Phe mutant. *J. Phys. Chem. B* **110**, 15 654–15 658. (doi:10.1021/jp063686b)
20. Woiczikowski PB, Steinbrecher T, Kubař T, Elstner M. 2011 Nonadiabatic QM/MM simulations of fast charge transfer in *Escherichia coli* DNA photolyase. *J. Phys. Chem. B* **115**, 9846–9863. (doi:10.1021/jp204696t)
21. Aubert C, Vos MH, Mathis P, Eker APM, Brettel K. 2000 Intraprotein radical transfer during photoactivation of DNA photolyase. *Nature* **405**, 586–590. (doi:10.1038/35014644)
22. Davidson VL, Liu AM. 2012 Tryptophan tryptophylquinone biosynthesis: a radical approach to posttranslational modification. *Biochim. Biophys. Acta* **1824**, 1299–1305. (doi:10.1016/j.bbapap.2012.01.008)
23. Geng JF, Dornevil K, Davidson VL, Liu AM. 2013 Tryptophan-mediated charge-resonance stabilization in the *bis*-Fe(IV) redox state of MauG. *Proc. Natl Acad. Sci. USA* **110**, 9639–9644. (doi:10.1073/pnas.1301544110)
24. Yukl ET, Liu FG, Krzystek J, Shin S, Jensen LMR, Davidson VL, Wilmot CM, Liu A. 2013 Diradical intermediate within the context of tryptophan tryptophylquinone biosynthesis. *Proc. Natl Acad. Sci. USA* **110**, 4569–4573. (doi:10.1073/pnas.1215011110)
25. Davidson VL, Wilmot CM. 2013 Posttranslational biosynthesis of the protein-derived cofactor tryptophan tryptophylquinone. *Annu. Rev. Biochem.* **82**, 531–550. (doi:10.1146/annurev-biochem-051110-133601)
26. Jiang N, Kuznetsov A, Nocek JM, Hoffman BM, Crane BR, Hu XQ, Beratan DN. 2013 Distance-independent charge recombination kinetics in cytochrome *c*–cytochrome *c* peroxidase complexes: compensating changes in the electronic coupling and reorganization energies. *J. Phys. Chem. B* **117**, 9129–9141. (doi:10.1021/jp401551t)
27. Wallrapp FH, Voityuk AA, Guallar V. 2013 In-silico assessment of protein–protein electron transfer. A case study: cytochrome *c* peroxidase–cytochrome *c*. *PLoS Comput. Biol.* **9**, e1002990. (doi:10.1371/journal.pcbi.1002990)
28. Butchosa C, Simon S, Voityuk AA. 2010 Electron transfer from aromatic amino acids to guanine and adenine radical cations in π stacked and T-shaped complexes. *Org. Biomol. Chem.* **8**, 1870–1875. (doi:10.1039/b927134a)
29. Shih C *et al*. 2008 Tryptophan-accelerated electron flow through proteins. *Science* **320**, 1760–1762. (doi:10.1126/science.1158241)
30. Blanco-Rodriguez AM *et al*. 2011 Phototriggering electron flow through Re^{I}-modified *Pseudomonas aeruginosa* azurins. *Chem. Eur. J.* **17**, 5350–5361. (doi:10.1002/chem.201002162)
31. Warren JJ, Ener ME, Vlèek A, Winkler JR, Gray HB. 2012 Electron hopping through proteins. *Coord. Chem. Rev.* **256**, 2478–2487. (doi:10.1016/j.ccr.2012.03.032)
32. Takematsu K *et al*. 2013 Tryptophan-accelerated electron flow across a protein–protein interface. *J. Am. Chem. Soc.* **134**, 15 515–15 525. (doi:10.1021/ja406830d)
33. Warren JJ, Herrera N, Hill MG, Winkler JR, Gray HB. 2013 Electron flow through nitrotyrosinate in *Pseudomonas aeruginosa* azurin. *J. Am. Chem. Soc.* **135**, 11 151–11 158. (doi:10.1021/ja403734n)
34. Renaud N, Berlin YA, Lewis FD, Ratner MA. 2013 Between superexchange and hopping: an intermediate charge-transfer mechanism in poly(A)-poly(T) DNA hairpins. *J. Am. Chem. Soc.* **135**, 3953–3963. (doi:10.1021/ja3113998)
35. Zhang Y, Liu C, Balaeff A, Skourtis SS, Beratan DN. 2014 Biological charge transfer via flickering resonance. *Proc. Natl Acad. Sci. USA* **111**, 10 049–10 054. (doi:10.1073/pnas.1316519111)
36. Marcus RA, Sutin N. 1985 Electron transfers in chemistry and biology. *Biochim. Biophys. Acta* **811**, 265–322. (doi:10.1016/0304-4173(85)90014-X)
37. Hammes-Schiffer S, Stuchebrukhov AA. 2010 Theory of coupled electron and proton transfer reactions. *Chem. Rev.* **110**, 6939–6960. (doi:10.1021/cr1001436)

38. Migliore A, Polizzi NF, Therien MJ, Beratan DN. 2014 Biochemistry and theory of proton-coupled electron transfer. *Chem. Rev.* **114**, 3381–3465. (doi:10.1021/cr4006654)
39. Weinberg DR *et al*. 2012 Proton-coupled electron transfer. *Chem. Rev.* **112**, 4016–4093. (doi:10.1021/cr200177j)
40. Gray HB, Winkler JR. 2010 Electron flow through metalloproteins. *Biochim. Biophys. Acta* **1797**, 1563–1572. (doi:10.1016/j.bbabio.2010.05.001)
41. Winkler JR, Gray HB. 2014 Electron flow through metalloproteins. *Chem. Rev.* **114**, 3369–3380. (doi:10.1021/cr4004715)
42. Winkler JR, Gray HB. 2014 Long-range electron tunneling. *J. Am. Chem. Soc.* **136**, 2930–2939. (doi:10.1021/ja500215j)
43. Denisov IG, Makris TM, Sligar SG, Schlichting I. 2005 Structure and chemistry of cytochrome P450. *Chem. Rev.* **105**, 2253–2277. (doi:10.1021/cr0307143)
44. Whitehouse CJC, Bell SG, Wong LL. 2012 $P450_{BM3}$ (CYP102A1): connecting the dots. *Chem. Soc. Rev.* **41**, 1218–1260. (doi:10.1039/c1cs15192d)
45. Johnson EF, Stout CD. 2013 Structural diversity of eukaryotic membrane cytochrome P450s. *J. Biol. Chem.* **288**, 17 082–17 090. (doi:10.1074/jbc.R113.452805)
46. Amdursky N, Molotskii M, Gazit E, Rosenman G. 2010 Elementary building blocks of self-assembled peptide nanotubes. *J. Am. Chem. Soc.* **132**, 15 632–15 636. (doi:10.1021/ja104373e)
47. Hauser CAE, Zhang SG. 2010 Nanotechnology: peptides as biological semiconductors. *Nature* **468**, 516–517. (doi:10.1038/468516a)
48. Vargas M, Malvankar NS, Tremblay PL, Leang C, Smith JA, Patel P, Snoeyenbos-West O, Nevin KP, Lovley DR. 2013 Aromatic amino acids required for pili conductivity and long-range extracellular electron transport in *Geobacter sulfurreducens*. *mBio* **4**, e00270-13. (doi:10.1128/mBio.00210-13)
49. Girvan HM, Seward HE, Toogood HS, Cheesman MR, Leys D, Munro AW. 2007 Structural and spectroscopic characterization of P450 BM3 mutants with unprecedented P450 heme iron ligand sets—new heme ligation states influence conformational equilibria in P450 BM3. *J. Biol. Chem.* **282**, 564–572. (doi:10.1074/jbc.M607949200)
50. Munro AW, Malarkey K, McKnight J, Thomson AJ, Kelly SM, Price NC, Lindsay JC, Coggins JR, Miles JS. 1994 The role of tryptophan-97 of cytochrome P450 BM3 from *Bacillus megaterium* in catalytic function—evidence against the 'covalent switching' hypothesis of P450 electron-transfer. *Biochem. J.* **303**, 423–428.
51. Denisov IG, Baas BJ, Grinkova YV, Sligar SG. 2007 Cooperativity in cytochrome P450 3A4: linkages in substrate binding, spin state, uncoupling, and product formation. *J. Biol. Chem.* **282**, 7066–7076. (doi:10.1074/jbc.M609589200)
52. Grinkova YV, Denisov IG, McLean MA, Sligar SG. 2013 Oxidase uncoupling in heme monooxygenases: human cytochrome P450 CYP3A4 in nanodiscs. *Biochem. Biophys. Res. Commun.* **430**, 1223–1227. (doi:10.1016/j.bbrc.2012.12.072)
53. Staudt H, Lichtenb F, Ullrich V. 1974 Role of NADH in uncoupled microsomal monoxygenations. *Eur. J. Biochem.* **46**, 99–106. (doi:10.1111/j.1432-1033.1974.tb03601.x)
54. Puntarulo S, Cederbaum AI. 1998 Production of reactive oxygen species by microsomes enriched in specific human cytochrome P450 enzymes. *Free Rad. Biol. Med.* **24**, 1324–1330. (doi:10.1016/S0891-5849(97)00463-2)
55. De Matteis F, Dawson SJ, Pons N, Pipino S. 2002 Bilirubin and uroporphyrinogen oxidation by induced cytochrome P4501A and cytochrome P4502B—role of polyhalogenated biphenyls of different configuration. *Biochem. Pharmacol.* **63**, 615–624. (doi:10.1016/S0006-2952(01)00851-6)
56. De Matteis F, Ballou DP, Coon MJ, Estabrook RW, Haines DC. 2012 Peroxidase-like activity of uncoupled cytochrome P450: studies with bilirubin and toxicological implications of uncoupling. *Biochem. Pharmacol.* **84**, 374–382. (doi:10.1016/j.bcp.2012.04.016)